

From Siderophores and Self-Assembly to Luminescent Sensors: The Binding of Molybdenum by Catecholamides

Anne-K. Duhme-Klair*^[a]

Keywords: Molybdenum / Siderophores / Self-assembly / Bioinorganic chemistry / Luminescent sensors

Molybdate reacts readily and instantly with 2,3-dihydroxybenzamide-containing ligands (catecholamides) to give stable *cis*-dioxido-Mo^{VI} complexes. This reaction is of biological relevance, because it results in the competition of molybdate with Fe^{III} for siderophores of the catecholamide type. These siderophores are secreted by bacteria to acquire essential Fe^{III} and help the cells to cope with variations in metal ion concentrations in their environment. This microreview summarises the insights obtained in this area and

analyses the structures of the Mo^{VI} complexes formed. In addition, the scope of the structure-defining potential of the *cis*-dioxido-Mo^{VI} unit in the self-assembly of supramolecular structures is illustrated. The final part of the review describes how catecholamide units can be used in the development of luminescent chemosensors for molybdate.

(© Wiley-VCH Verlag GmbH & Co. KGaA, 69451 Weinheim, Germany, 2009)

Introduction

Due to its versatile coordination chemistry, molybdenum plays an important role in biology^[1] as well as industry.^[2] Under aerobic conditions and in oxic environments, molybdenum is mainly present in its highest oxidation state, Mo^{VI}, with d⁰ configuration. In aqueous solution, hydrolysis leads to the formation of a variety of oxometalates, the speciation of which depends on pH and concentration. Whilst under acidic conditions proton-induced condensation reactions lead to the generation of polyoxomolybdates, the predominating species formed in dilute solutions near neutral pH is the mononuclear, tetrahedral oxodianion molybdate (MoO₄²⁻).^[3,4] In the presence of organic chelate ligands, the molybdenum can enhance its coordination number to up to six to form distorted octahedral dioxidomolybdenum complexes (Figure 1). In these complexes, the two strong π -donating oxido ligands are generally found in *cis* orientation, because this geometry allows interactions with three molybdenum d π orbitals, thereby maximising π -bonding (Figure 2).^[5–7] Accordingly, unsymmetrical chelate ligands, such as 2,3-dihydroxybenzoic acid^[8] and 2,3-dihy-

droxybenzamides (catecholamides), coordinate preferentially with the weaker donor positioned *trans* to the oxido ligands to avoid competition for the same d orbitals.

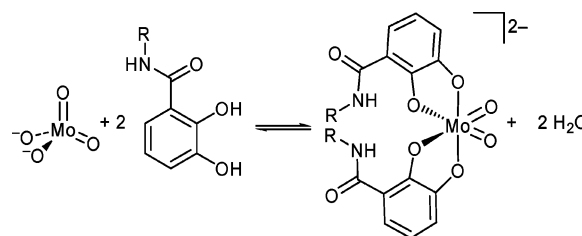


Figure 1. The reaction of molybdate with catecholamides.

Many of the early studies on Mo^{VI} catecholamide complexes were motivated by the observation that molybdate competes with Fe^{III} for catecholamide-siderophores, which are small molecule chelators produced by microorganisms to acquire Fe^{III} from their environment. Because this area has recently attracted renewed interest, the first part of this microreview summarises the insights obtained into the affinity of catecholamide siderophores for these biometals to date. The second part of the review focuses on the struc-

[a] Department of Chemistry, University of York, York, YO10 5DD, UK



Anne-Kathrin Duhme-Klair is a senior lecturer in the Department of Chemistry at the University of York. She obtained her PhD in the area of bioinorganic chemistry at the University of Oldenburg, Germany. After postdoctoral positions at King's College London, the European Molecular Biology Laboratory at DESY in Hamburg and the Nitrogen Fixation Laboratory at the John Innes Centre in Norwich, she completed her habilitation in inorganic chemistry at the University of Münster under the supervision of Professor Bernt Krebs. She joined the Chemistry Department in York as a lecturer in biological inorganic chemistry in 1998. Her current research interests include the coordination chemistry of siderophores, metal-based luminescent probes and metal-containing drugs.

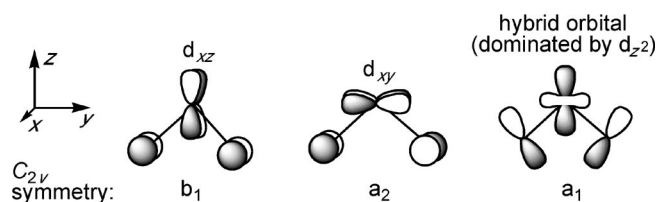


Figure 2. Schematic illustration of the d and p orbitals involved in π -interactions between Mo^{VI} and the two oxido ligands in a *cis*- MoO_2^{2+} unit (modified from ref.[5]).

tures of Mo^{VI} complexes and the molecular recognition directing properties of the *cis*-dioxido- Mo^{VI} unit in the self-assembly of di- and trinuclear catecholamide complexes. The final part of the review describes how the design features used by catecholamide siderophores to discriminate Fe^{III} from Mo^{VI} can be exploited in the development of luminescent chemosensors for oxometalates, such as molybdate.

Complexation of Molybdenum by Catecholamide Siderophores

The reaction of molybdate with catecholamides leads to the immediate formation of orange-coloured complexes. These are apparent and easily detectable in the culture supernatant of *Azotobacter vinelandii*.^[9,10] This nitrogen-fixing soil bacterium produces and secretes at least three different catecholamide siderophores in response to different metal-ion concentrations (Figure 3).^[11,12] As both iron and molybdenum are components of the cofactor of the conventional nitrogenase, the hypothesis that catecholamide siderophores produced by nitrogen-fixing bacteria may not only be involved in the acquisition of Fe^{III} but also in the mediation of Mo^{VI} uptake has attracted considerable interest. For comprehensive reviews on bacterial molybdenum uptake see Shanmugam 1997,^[13] Pau and Lawson, 2002^[14] and Pau, 2004.^[15]

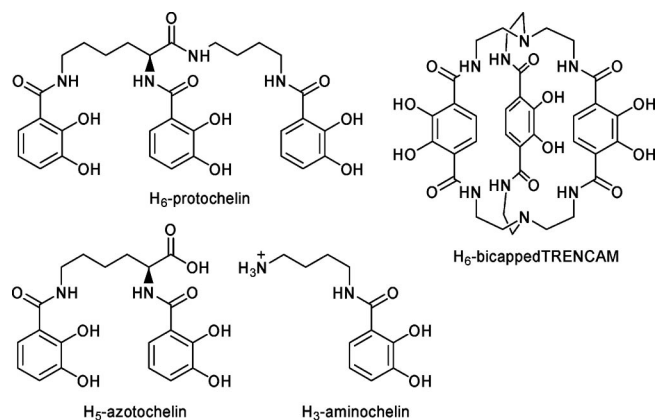


Figure 3. Structures of the catecholamide siderophores produced by *Azotobacter vinelandii* (left) and the macrobicyclic ligand H_6 -bicapped TRENCAM (right).

Protochelin

Of the siderophores produced by *A. vinelandii*, only the tris(catecholamide) siderophore protochelin exhibits the typical hexadentate structure of bacterial siderophores, such as enterobactin of *E. coli*.^[16] Therefore, protochelin is a very efficient siderophore and able to solubilise freshly precipitated iron hydroxide rapidly (Figure 4).^[17] Protochelin binds Fe^{III} with high affinity to give the 1:1 complex $[\text{Fe}(\text{protochelin})]^{3-}$. With a $\log K_{(\text{FeL})}$ value of approximately 44,^[17,18] the proton independent stability constant of the protochelin complex is very similar to that reported for the linear form of enterobactin [$\log K_{(\text{FeL})}$ of 43].^[19] Interestingly, protochelin can only be found in the growth medium if either competing metal ions or chelate ligands compromise the binding of Fe^{III} by the lower denticity siderophores azotochelin and amino chelin. Examples include the presence of toxically high levels of oxometalates, such as molybdate^[11,12] or tungstate,^[20,21] metal cations, such as Zn^{II} or Mn^{II} ,^[20] or the presence of iron chelators, such as EDTA.^[21,22]

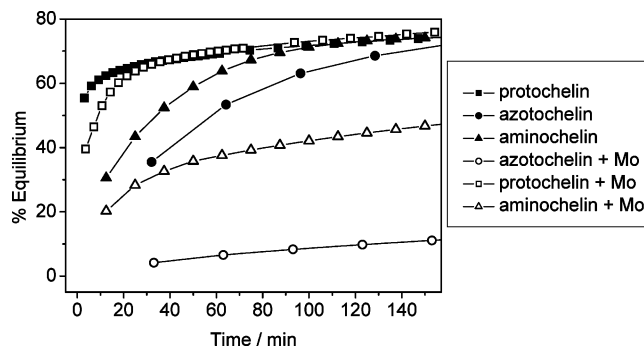


Figure 4. Time course of the siderophore-mediated solubilisation of iron(III) hydroxide in the absence and presence of an equimolar amount of molybdate at neutral pH.

Molybdate reacts with H_6 -protochelin to form a molybdenum(VI) complex of composition $[\text{MoO}_2(\text{H}_2\text{-protochelin})]^{2-}$, as has recently been shown by ESI mass spectrometry.^[22] In the complex, H_2 -protochelin is likely to bind as a tetradentate ligand with one of the catecholamide units remaining uncoordinated. A similar arrangement was observed in the crystal structure of $[\text{MoO}_2(\text{H}_2\text{-bicapped-TRENCAM})]^{2-}$ (Figure 3), in which the macrobicyclic tris(catecholate) acts as a tetradentate ligand and one terephthalamide unit remains uncoordinated.^[23] It is thus the third catecholamide unit and the resulting hexadentate structure that makes protochelin a more efficient iron chelator than the tetradentate azotochelin (vide infra).

Azotochelin

The tetradentate structure of the bis(catecholamide) siderophore azotochelin matches the coordination requirements of the *cis*- MoO_2^{2+} unit, which has four vacant coordination sites.^[24] Near neutral pH, the *cis*-dioxido- Mo^{VI} complex $[\text{MoO}_2(\text{azotochelin})]^{3-}$ is formed, which was characterised by ESI mass spectrometry,^[12] ^1H NMR spectroscopy^[25] and X-ray absorption spectroscopy.^[26] As no

protons are released or consumed during the reaction of molybdate with azotochelin around neutral pH (Figure 1), the complex formation cannot be detected potentiometrically. The affinity of the ligand for molybdenum was therefore assessed via spectrophotometric determinations of the apparent equilibrium constant.^[12,20,26] The reported $\log K_{\text{eq}}$ values range from 3.6 ± 0.06 ^[20] to 7.6 ± 0.4 .^[26]

Azotochelin cannot form coordinatively saturated 1:1 complexes with octahedral Fe^{III} . As azotochelin is only tetradentate, it requires additional ligands to form six-coordinate Fe^{III} complexes. A pH dependent equilibrium involving a dinuclear complex with azotochelin to Fe^{III} ratio of 3:2 and a mononuclear azotochelin bis(aqua) Fe^{III} complex is thus conceivable, as observed for structurally related bis(catecholamides), such as the amonabactins of *Aeromonas hydrophila*.^[27] A potentiometric determination of the stability constant of the iron azotochelin complex has recently been attempted, but proved difficult due to slow equilibration.^[26]

Although azotochelin is able to solubilise iron oxides and iron hydroxides,^[28] it is not a particularly efficient siderophore as it takes almost two hours to solubilise half an equivalent of freshly precipitated iron hydroxide. Interestingly, the solubilisation is delayed by a factor of 23 in the presence of molybdate, with the iron complex reaching half of its final concentration only after almost two days.^[29] It is therefore not surprising that azotochelin is only produced by *A. vinelandii* to sequester available iron if grown at low molybdate levels. If molybdate levels in the growth medium increase to a concentration that approaches the concentration of the secreted azotochelin (around $100 \mu\text{M}$), the azotochelin production stops and protochelin is produced instead.^[11,12] If this switch would not occur, the quantitative formation of the $[\text{MoO}_2(\text{azotochelin})]^{3-}$ complex would drastically reduce the iron-solubilising ability of the siderophore. The hexadentate ligand protochelin, on the other hand, is more efficient as an iron chelator, in particular in the presence of an equimolar amount of molybdate. In this case the solubilisation of iron hydroxide is delayed only by a factor of five (Figure 4).^[17] This is likely to be due to the uncoordinated catecholamide unit in $[\text{MoO}_2(\text{H}_2\text{-protochelin})]^{2-}$, which remains available for iron binding.^[17]

Azotochelin is not suitable for the extraction of molybdenum from Mo-containing silicates either, as it was observed to repress rather than enhance the release of Mo from glass.^[30] Because the carboxylic acid group of azotochelin is deprotonated at neutral pH and silicate glass surfaces acquire a negative surface charge in water at this pH due to the dissociation of terminal silanol groups,^[31] electrostatic repulsion of the negatively charged siderophore may contribute to this effect. Aminochelin, which is positively charged at neutral pH, was seen to enhance the release of Mo under analogous conditions,^[30] as described in more detail below.

Aminochelin

The metal-binding properties of the unusual mono(catecholamide) siderophore aminochelin are particularly inter-

esting. This is mainly due to the hydrophilicity of the pendant amine group, which is protonated at neutral pH, and the resulting zwitterionic character of its complexes $[\text{Fe}(\text{H-aminochelin})_3]^{32}$ and $[\text{MoO}_2(\text{H-aminochelin})_2]^{32,33}$ (Figure 5). Based on a spectrophotometric competition study with EDTA, the proton-independent overall stability constant for the Fe^{III} aminochelin 1:3 complex was estimated as $\log \beta_{(\text{FeL}_3)} = 41.3$.^[32] Despite being only bidentate, aminochelin is able to function as a siderophore as it was seen to mediate the uptake of $^{55}\text{Fe}^{\text{III}}$ into *A. vinelandii* cells.^[34] In addition, the initial rate of iron hydroxide solubilisation by aminochelin is surprisingly fast (Figure 4). Half of the equilibrium Fe^{III} complex concentration is already reached within 30 min. Molybdate addition delays the process ($t_{1/2} = 3.5 \text{ h}$), but the delay is far less pronounced than in the case of azotochelin.^[32]

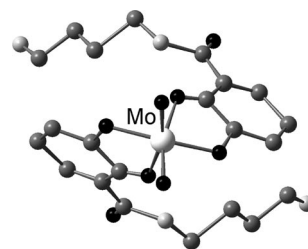


Figure 5. Ball-and-stick representation of the molecular structure of $[\text{MoO}_2(\text{H-aminochelin})_2]$. O black, N light grey, C grey, Mo white, H atoms omitted for clarity. The butyl chains are heavily disordered over more than two alternative positions, only one of the possibilities is shown.

Interestingly, it was recently observed that aminochelin is still produced even if the iron levels are high, provided that the growth medium is deficient in molybdate.^[30] Aminochelin was also identified as the siderophore (and potential “molybdophore”) that is responsible for the increased release of molybdate from glass observed in the presence of *A. vinelandii* cells.^[30] The addition of glass proved to be particularly beneficial for cells that were forced to fix nitrogen, which increases their requirement for iron and molybdenum drastically.

One mechanism suggested for the intracellular release of sequestered iron from its siderophore complex is the enzymatic reduction of Fe^{III} to Fe^{II} , which triggers a decrease in the stability of the complex and therefore dissociation.^[35,36] The first reported example of a specific reductase for iron–siderophore complexes is the cytoplasmic protein FhuF of *E. coli*.^[37] While FhuF reduces the Fe^{III} complexes of hydroxamate siderophores, the recently identified FerA enzyme of *Paracoccus denitrificans* triggers the reductive release of iron from the bis(catecholamide) siderophore parabactin.^[38] In order to investigate whether molybdenum–bis(catecholamide) complexes can undergo a similar reduction, the electrochemistry of $[\text{MoO}_2(\text{H}_2\text{-protochelin})]^{2-}$, $[\text{MoO}_2(\text{azotochelin})]^{3-}$ and $[\text{MoO}_2(\text{H-aminochelin})_2]$ was investigated at pH 6.74 in pyridine buffer.^[39] Two sequential reduction steps were observed: $\text{Mo}^{\text{VI}} \rightarrow \text{Mo}^{\text{V}}$ at potentials between -0.2 and -0.3 V and $\text{Mo}^{\text{V}} \rightarrow$

Mo^{III} at potentials between -0.5 and -0.55 V vs. NHE. For comparison, the reduction potential of the Fe^{III} –parabactin complex is -0.67 V vs. NHE at pH 7.0.^[40] In the presence of coordinating ligands, such as pyridine, the reduction of Mo^{VI} in catecholamide complexes is thus easier to achieve than the reduction of Fe^{III} in the parabactin complex. The siderophore-chelated Mo^{VI} could even be reduced to Mo^{V} by biological reducing agents such as NAD(P)H or flavins.

The evidence is thus mounting that the catecholamide siderophores of *A. vinelandii* do not only mediate bacterial iron uptake but are also affecting the uptake of oxometalates, such as molybdate. In how far they may be involved, directly or indirectly, in the cellular uptake and transport of molybdenum is discussed below.

Implications for Bacterial Molybdenum Uptake

Molybdenum uptake in *A. vinelandii* is fast; under nitrogen-fixing conditions, the growth medium can be depleted of molybdate within one hour.^[41] Because the catecholamide siderophores, once secreted, chelate the available molybdenum instantly and almost quantitatively, the cells must have a molybdenum uptake system that allows them to acquire the essential element from its siderophore complexes. That ^{95}Mo supplied in the form of isotopically lab-

elled azotochelin and protochelin complexes is taken up by the cells has recently been confirmed by inductively coupled plasma mass spectrometry (ICP-MS).^[22] The question remains in which form the molybdenum crosses the outer membrane of the cell. Because the siderophore complexes are too large to fit through porin channels, specific receptor proteins are required to transport the complexes into the periplasm, unless the molybdenum complexes are recognised and transported by the corresponding iron–siderophore receptor proteins (Figure 6). Thus far, specific receptor proteins for molybdenum–siderophore complexes have not been identified. It is, however, documented that in the periplasm, molybdate is sequestered by its periplasmic binding protein ModA,^[13,14,42–44] which delivers the molybdate to the inner membrane transporter for translocation into the cytoplasm.^[14,15,45] Crystal structure determinations showed that the molybdate-binding hydrogen bond arrangement in ModA proteins from *E. coli*, *A. vinelandii*, *Archaeoglobus fulgidus* and *Xanthomonas axonopodis* is very similar, despite differences in amino acid sequences.^[46] The apparent dissociation constant for molybdate binding by ModA of *E. coli* is 20 nM,^[47] which equates to an apparent equilibrium constant $\log K_{\text{eq}}$ of 7.70. If the molybdate affinity of the *A. vinelandii* ModA protein were to be similar to the affinity of the *E. coli* protein, a quantitative transfer of

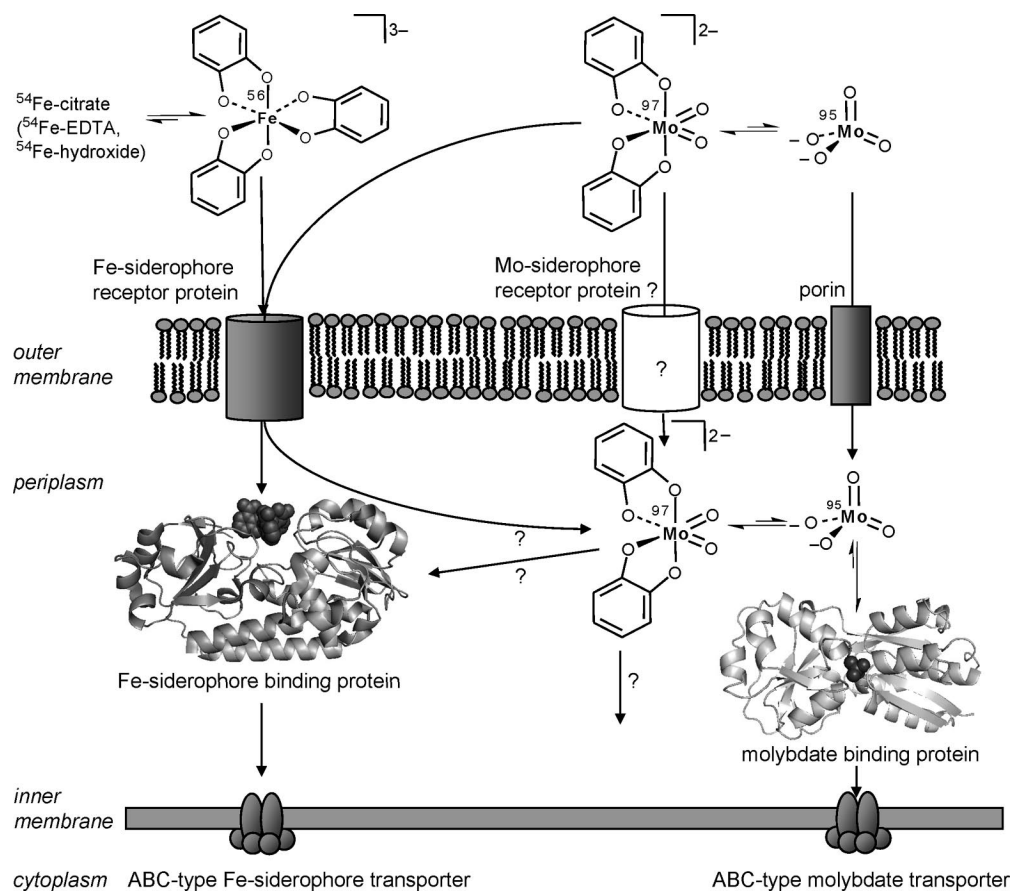


Figure 6. Schematic representation of conceivable routes for the uptake of Mo^{VI} into a gram-negative bacterial cell. The isotopes are indicated only to illustrate trends that are expected due to thermodynamic isotope effects. PDB codes of protein structures used: 2CHU^[49] and 1AMF.^[44] The protein-bound molybdate and iron(III)–tris(catecholate) are shown in space-fill representation.

molybdenum from a siderophore complex to ModA would only be possible for complexes that have a significantly lower $\log K_{\text{eq}}$ value than that of ModA at the pH of the periplasm. A specific periplasmic binding protein for molybdenum–siderophore complexes has not yet been found.

Evidence for a change in the coordination sphere of molybdenum in the course of the bacterial uptake process could recently be obtained from high precision isotopic analyses. While the lighter isotopes of molybdenum were taken up preferentially by the cells, the heavier isotopes accumulated in the growth medium. Depending on the growth conditions chosen, $\Delta^{97/95}\text{Mo}_{\text{cells-medium}}$ values of -0.3% ^[48] to -0.6% ^[30] were obtained. Such an isotope fractionation is consistent with the kinetic isotope effect accelerating the rate of ^{95}Mo uptake. In addition, thermodynamic isotope effects could play a role if equilibria between different species in the medium and/or the periplasm are involved, which would favour the partitioning of ^{97}Mo into the species in which it is most strongly bound, for example into a stable catecholamide complex.

Interestingly, the fractionation of iron isotopes shows the opposite trend. The heavier isotopes are taken up preferentially and the lighter isotopes accumulate in the growth medium ($\Delta^{56/54}\text{Fe}_{\text{cells-medium}} = 1.1\%$).^[48] Consequently, the iron uptake process is dominated by a thermodynamic isotope effect, suggesting that the Mo- and Fe-uptake mechanisms differ in at least one step. Assuming that equilibrium fractionation would lead to the heavier isotopes of both Fe and Mo partitioning into their respective siderophore complexes, the difference must be related to the cellular transport mechanisms. In gram-negative bacteria, the iron–siderophore complexes cross the outer membrane intact and are captured as such by specific periplasmic binding proteins,^[49] which deliver them to the inner membrane transporter. In contrast, molybdenum is bound as molybdate by its periplasmic binding protein ModA. Molybdenum uptake thus requires the release of molybdate from its siderophore complex for ModA binding and further transport to occur. This should result in preferential sequestration of the lighter isotopes for kinetic as well as thermodynamic reasons and is consistent with the observed isotope distribution. These considerations are summarised in Figure 6. Surface-adsorption effects, however, may also cause isotope fractionation. Further studies are thus thought necessary in order to differentiate the effects.^[48]

If taken together, the molybdenum- and iron-binding studies carried out on the siderophores produced by *A. vinelandii* have revealed complex structure affinity relationships. These point towards a very subtle regulation of metal uptake that helps the cells to respond to variations in metal ion concentrations in their environment.^[50]

The identification of the design features that allow these siderophores to differentiate between different bioessential metal ions has also contributed to the understanding of the supramolecular chemistry of catecholamide ligands and inspired the use of catecholamide-based receptor units in chemosensors for oxometallates, as described in the following two sections.

The Structures of Molybdenum–Catecholamide Complexes

Upon coordination of two asymmetrically substituted catecholate units to a *cis*-dioxidomolybdenum(VI) centre, three *cis/trans* isomers can be formed in either Δ or Λ configuration, as illustrated in Figure 7 and Figure 8. Due to the strong *trans* influence of the two oxido ligands, the thermodynamically favoured geometrical isomer is the *cis, trans, cis* isomer, in which the weaker donor in the 2-position of the catecholamide is coordinated *trans* to the oxido ligands. This is the isomer seen in the solid-state structures of complexes with bidentate ligands, such as $[\text{MoO}_2(\text{dhb})_2]^{2-}$ ($\text{H}_2\text{-dhb} = 2,3\text{-dihydroxybenzoic acid}$),^[51] $[\text{MoO}_2(\text{L}^{\text{6a}})_2]^{2-}$ ($\text{H}_2\text{-L}^{\text{6a}}$: Figure 9),^[52] and $[\text{MoO}_2(\text{H-aminochelin})_2]$.^[33] The energetic difference between isomers **a** and **b**, however, is not large and mixtures can be formed in solution. For $[\text{MoO}_2(\text{dhb})_2]^{2-}$, for example, a variable temperature proton NMR study in deuterated methanol revealed an **a/b/c** ratio of approximately 1:2:0.^[51]

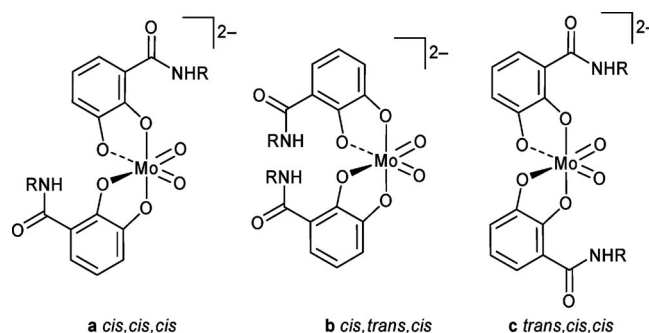


Figure 7. Conceivable geometric isomers of *cis*-dioxidomolybdenum(VI) complexes with two catecholamide ligands shown in Λ configuration. The *cis/trans* assignments refer to the following order: phenolate donor in the 2-position, phenolate donor in the 3-position, oxido ligand.

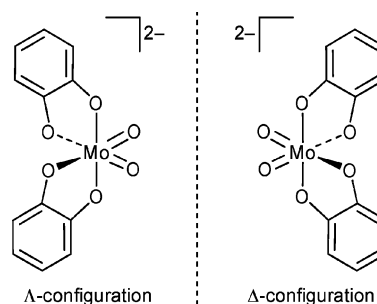


Figure 8. The two optical isomers formed upon coordination of two catecholamide ligands to a *cis*-dioxidomolybdenum(VI) unit.

If the two coordinating catecholamide units are connected through a linker, as in the ligands shown in Figure 9, steric constraints can determine the type of geometric isomer formed. As evident from the crystal structure of $[\text{MoO}_2(\text{L}^1)]^{2-}$ (Figure 10),^[53] a mononuclear complex in which one ligand coordinates to the MoO_2^{2+} centre has to adopt *cis, cis, cis* geometry, as this positions the two amide groups of the catecholamide units at a suitable distance for bis(bidentate) chelation to occur.

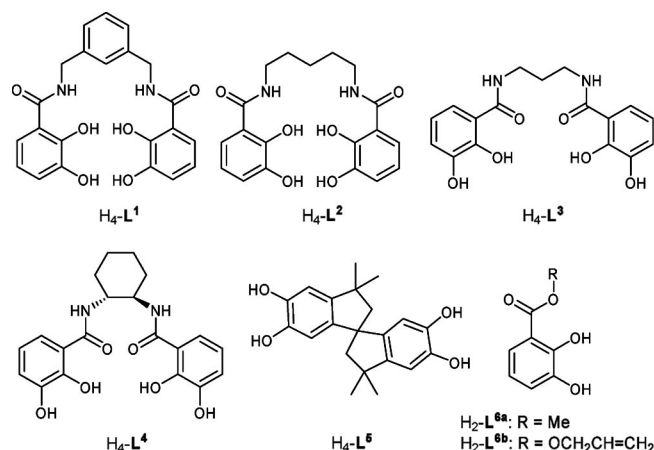
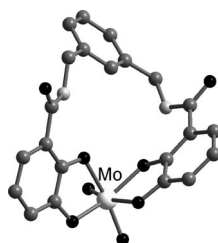
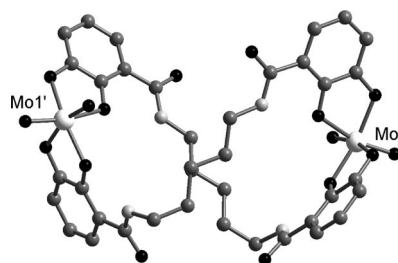


Figure 9. Ligand structures.

Figure 10. Structure of $[\text{MoO}_2(\text{L}^1)]^{2-}$. O black, N light grey, C grey, Mo white, H atoms omitted for clarity.

Bis(catecholamide) ligands, however, can also be used in the preparation of dinuclear and even multinuclear metal complexes. The structures of the resulting supramolecular complexes depend on the type of linker that connects the coordinating catecholate units. The principles that govern such metal-directed self-assembly processes are now well understood.^[54–57,58]

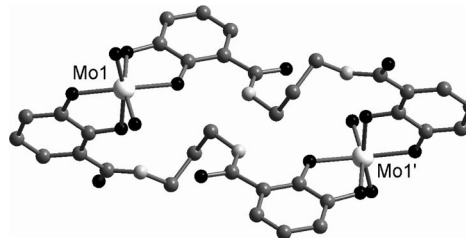
The reaction of molybdate with $\text{H}_4\text{-L}^1$ initially leads to the formation of a dinuclear 2:2 complex, which converts into the entropically favoured mononuclear 1:1 complex $[\text{MoO}_2(\text{L}^1)]^{2-}$ upon prolonged heating in dmsu.^[53] Due to the rigidity of the aromatic linker, the dissociation is not reversible upon cooling. In case of the related ligand $\text{H}_4\text{-L}^2$ (Figure 9), the corresponding 2:2 complex, $[\{\text{MoO}_2(\text{L}^2)\}_2]^{4-}$, could be crystallised. X-ray diffraction revealed the structure of a dinuclear double-stranded helicate (Figure 11),^[59] which was one of the first catecholate-based helicates to be structurally characterised.^[60–62] Again the *cis,cis,cis* isomer is present in the solid state, as it allows the dimerisation. A variable temperature proton NMR study in deuterated methanol confirmed the presence of the *cis,cis,cis* isomer at low temperature, whilst broad resonances were observed at room temperature. Further heating indicated complex dynamic behaviour: symmetrisation of the diastereotopic methylene protons due to inversion of configuration and changes in the aromatic region of the spectrum due to geometric isomerisation and potentially dissociation. In this case cooling restored the original spectrum.^[59]

Figure 11. Ball-and-stick representation of the structure of $\Delta,\Lambda\text{-}[\{\text{MoO}_2(\text{L}^2)\}_2]^{4-}$, O black, N light grey, C grey, Mo white, H atoms omitted for clarity.

Because the coordinating catecholamide groups in $\text{H}_4\text{-L}^1$ and $\text{H}_4\text{-L}^2$ both have 5-atomic spacing that resembles the lysine backbone of azotochelin, their complexes may be regarded as models of the *cis*- MoO_2^{2+} complex of the siderophore. The azotochelin complex, however, is most likely to be mononuclear, due to the additional negative charge provided by the carboxylate group. A mononuclear complex is also consistent with the molecular ion observed in the ESI mass spectrum.

The double-helical structure of $[\{\text{MoO}_2(\text{L}^2)\}_2]^{4-}$ is unusual as it differs from the double-helical structures that are obtained upon coordination of bis(bidentate) ligands to tetrahedral metal ions. It has since inspired further studies into the stereoelectronic preferences of the *cis*-dioxido- Mo^{VI} unit and in particular its potential in the self-assembly of other supramolecular structures.

If the chain length of the linker is reduced from five to three methylene groups, as in ligand $\text{H}_4\text{-L}^3$ (Figure 9), a tetradentate chelation of the *cis*-dioxido- Mo^{VI} is no longer possible. Accordingly, the formation of the dinuclear 2:2 complex was observed in the solid state (Figure 12).^[63] Because the two metal centres in the complex are related by an inversion centre $\Delta,\Lambda\text{-}[\{\text{MoO}_2(\text{L}^3)\}_2]^{4-}$ is an achiral “mesocate”, in which the two coordination centres exhibit opposite absolute configurations. In addition to packing effects, this may be caused by the short linker giving rise to the apparent side-by-side orientation of the ligands. Variable-temperature proton NMR studies confirmed that the “mesocate” $\Delta,\Lambda\text{-}[\{\text{MoO}_2(\text{L}^3)\}_2]^{4-}$ is more rigid than the helicate $\Lambda,\Lambda\text{-}[\{\text{MoO}_2(\text{L}^2)\}_2]^{4-}$.

Figure 12. Ball-and-stick representation of the structure of $\Delta,\Lambda\text{-}[\{\text{MoO}_2(\text{L}^3)\}_2]^{4-}$, O black, N light grey, C grey, H atoms omitted for clarity.

The even shorter and conformationally restricted cyclohexyl linker in $\text{H}_2\text{-L}^4$ (Figure 9) leads to the self-assembly of a molecular triangle (Figure 13).^[64] In this structure,

Mo2 lies on a pseudo-twofold axis of symmetry, with the catecholamide units coordinated in *cis,trans,cis* orientation. In contrast, Mo1 and Mo3 adopt a *cis,cis,cis* arrangement in order to enable the formation of a cyclic structure. Regardless of the geometric isomer formed, all three molybdenum centres in the complex have Δ configuration, as may be expected in a complex of an enantiomerically pure ligand, such as H_2-L^4 . In aqueous solution, the metal centres in $\Delta, \Delta, \Delta-[MoO_2(L^4)]_3]^{6-}$ invert to form the more hydrophilic Λ -configured diastereomer, as indicated by circular dichroism (CD) spectroscopy. Interestingly, the visible region of the CD spectrum of the *cis*- MoO_2 complex of azotochelin mirrors that of the Λ -configured diastereomer of $[MoO_2(L^4)]_3]^{6-}$. Consequently, the predominant configuration of the molybdenum centre in the siderophore complex can be assigned as Δ ,^[64] the configuration that is also adopted by the iron(III) centre in the biologically active enterobactin complex, which is recognised stereoselectively by its outer membrane receptor protein FepA. The identical charge and similar shape of $\Delta-[MoO_2(azotochelin)]^{3-}$ and $\Delta-[Fe(enterobactin)]^{3-}$ suggest that the molybdenum–azotochelin complex may be recognised by iron–siderophore receptors, although experimental evidence for this hypothesis has not yet been obtained.

A comparison of selected bond lengths and angles in the *cis,cis,cis*-configured MoO_6 centres in $[MoO_2(L^1)]^{2-}$, $[MoO_2(L^2)]_2]^{4-}$, $[MoO_2(L^3)]_2]^{4-}$ and $[MoO_2(L^4)]_3]^{6-}$ (Table 1) shows that their geometry is similar despite the differences in the structure of the ligands. Drastic distortions due to steric constraints of the linkers were avoided through formation of multinuclear complexes. The kinetic

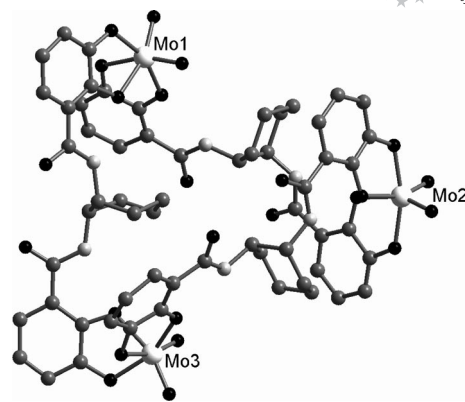
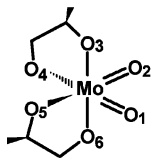


Figure 13. Ball-and-stick representation of the structure of $\Delta, \Delta, \Delta-[MoO_2(L^4)]_3]^{6-}$. O black, N light grey, C grey, Mo white, H atoms omitted for clarity.

lability of the Mo^{VI} centres allowed the formation of the thermodynamically most favourable product in each case. The *cis*- MoO_2 unit is thus a suitable building block in metal-directed self-assembly processes.

In addition, the two molybdenum-bound oxido ligands can be exploited for further intermolecular assembly processes, as they are often seen to interact with counter cations. This is evident from the solid-state structures of *cis*- MoO_2^{2+} complexes of structurally related catecholate ligands, such as the spiro ligand H_2-L^5 and the ester-substituted catecholates H_2-L^6 . In $[MoO_2(L^5)]_2]^{4-}$, the oxido ligands are part of a network consisting of sodium counterions and solvent oxygen donors that links the dinuclear mo-

Table 1. Comparison of selected bond lengths and angles in *cis*- MoO_2 catecholamide complexes (*cis/trans* assignments as in Figure 7).

		$[MoO_2(L^2)]_2]^{4-}$	$[MoO_2(L^1)]_2]^{2-}$	$[MoO_2(L^3)]_2]^{4-}$	$[MoO_2(L^4)]_3]^{6-}$ Mo1	$[MoO_2(L^4)]_3]^{6-}$ Mo3
Bond lengths /Å						
Mo–O1		1.719(4)	1.707(2)	1.734(3)	1.72(2)	1.70(2)
Mo–O2		1.717(4)	1.734(2)	1.711(3)	1.74(2)	1.69(2)
Mo–O3		1.996(3)	1.998(2)	2.032(3)	2.04(2)	2.01(2)
Mo–O4		2.114(4)	2.186(2)	2.117(3)	2.12(2)	2.14(2)
Mo–O5		2.137(4)	2.125(2)	2.212(3)	2.12(2)	2.15(2)
Mo–O6		2.005(3)	2.012(2)	1.989(3)	2.00(2)	2.04(2)
Bond angles /°						
O1–Mo–O2		101.7(2)	101.9(1)	102.7(2)	101.9(8)	103.2(8)
O3–Mo–O4		75.8(1)	75.3(1)	75.8(1)	75.5(8)	75.6(6)
O5–Mo–O6		75.3(1)	76.1(1)	74.8(1)	75.8(6)	75.3(7)
nuclearity:		dinuclear	mononuclear	dinuclear	trinuclear	trinuclear
geometric isomer		<i>cis,cis,cis</i>	<i>cis,cis,cis</i>	<i>cis,cis,cis</i>	<i>cis,cis,cis</i>	<i>cis,cis,cis</i>

lecular squares in the solid state (Figure 14).^[65] In $[\text{MoO}_2(\text{L}^{6a})_2]^{2-}$, an oxido ligand bridges between two lithium counterions that interact with the coordinated catecholate units,^[52] supporting dimerisation. The two dinuclear Mo complexes in $[\text{Li}_2\{(\mu\text{-O})(\mu\text{-DMF})\text{MoO}_2(\text{L}^{6b})\}_2(\text{DMF})_2]_2$ are linked in a similar way through interactions between terminal oxido ligands and lithium ions.^[52] These examples illustrate the scope of the *cis*- MoO_2^{2+} unit in the construction of hierarchical supramolecular systems.

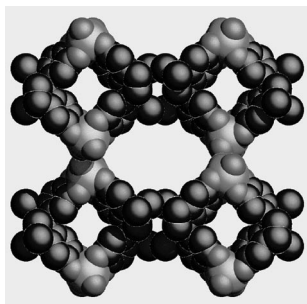


Figure 14. The packing of $[\{\text{MoO}_2(\text{L}^5)\}_2]^{4-}$ viewed down the *a* axis (Mo light grey, O grey, C black). H atoms, solvent molecules and counterions omitted for clarity.

The geometric and electronic preferences of the *cis*- MoO_2^{2+} unit have also been used for the spatial organisation of functionalised catecholate units. Supramolecular receptors for alkyl diammonium ions, for example, were obtained by coordination of two crown ether appended catecholate ligands to a *cis*- MoO_2^{2+} centre (Figure 15).^[66] Multiple hydrogen bonding and electrostatic attraction of the dicationic substrates by the dianionic receptor gives rise to binding constants ranging from $\log K = 3.5$ to 5.2. Only a slight preference for pentyl diammonium over butyl, hexyl, heptyl and octyl diammonium cations was observed, presumably due to the flexibility of both the substrates and the receptor. Similarly, a receptor for dicarboxylates was developed by connecting a thiourea-carrying group to a catecholate ligand. Formation of the *cis*- MoO_2^{2+} -dicatecholato complex yielded a receptor that recognises alkyl dicarboxylates ranging from succinate to pimelate with binding constants between $\log K$ 5.7 and 6.9.^[66]

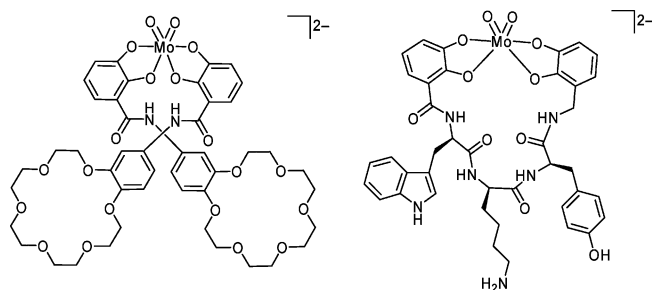


Figure 15. Structure of the diammonium receptor developed by Weiss et al.^[66] (left) and one of the metallacyclopeptides prepared by Albrecht et al.^[67] (right).

Inspired by the zinc finger proteins, in which Zn^{II} coordination to two histidine and two cysteine residues is a crucial structure-determining factor, the *cis*- MoO_2^{2+} unit has been

used in the preparation of metallacyclopeptides that mimic loop or turn type secondary structures.^[67] For this purpose, catecholate units were connected to both termini of biologically relevant tripeptide sequences and the resulting bis-(catecholate) ligands were coordinated to a *cis*- MoO_2^{2+} unit (Figure 15). A proton NMR spectroscopic investigation confirmed that the resulting metallacyclopeptides are conformationally restricted and that the side chains of tyrosine, aspartate, arginine, lysine and tryptophan are not involved in the molybdenum binding. This study opens up new avenues for the design of bio-selective complexes.

Luminescent Chemosensors for Molybdate

The extraordinary high affinity of catechol-based ligands^[68–72] and in particular catecholamides^[12,20,22] for molybdenum(VI) prompted us to investigate their application as metal-binding unit in luminescent chemosensors for oxometalates, such as molybdate, tungstate and vanadate. A fast and simple luminescence-based assay for these species is required for a range of analytical applications in environmental monitoring,^[73] biochemical research^[74] and medical analysis.^[75,76]

For analytical applications, high selectivity for molybdate over biologically important metal cations, such as Fe^{III} or Cu^{II} , and oxoanions, such as SO_4^{2-} and HPO_4^{2-} , is important. Selectivity over oxoanions can be achieved with catecholamide ligands, based on the unique coordination chemistry of molybdenum. While the molybdenum(VI) centre in molybdate is able to bind two catecholate ligands to enhance its coordination number to six, sulfur and phosphorus cannot react in this way. On the other hand, selectivity for oxometalates over cations, such as Fe^{III} , can be achieved by pH control (Figure 16). Whilst the reaction of molybdate with two catechol ligands leads to the release of two water molecules, the complexation of iron(III) by three catechol ligands liberates six protons. The latter is thus less favourable in acidic solutions. Because *cis*- MoO_2^{2+} -catecholate complexes have a characteristic orange colour whereas Fe^{III} -catecholate complexes are wine-red to purple, depending on pH, their speciation can be followed spectrophotometrically. However, because the ligand-to-metal charge-transfer band that is used for the colorimetric quantification of molybdenum-catecholate complexes is of rather low intensity the sensitivity of these methods is limited, with detection limits falling into the micromolar concentration range.^[77] In order to increase the sensitivity, we have connected luminophores with high quantum yields to catecholamide ligands (Figure 17) in order to develop chemosensors for molybdate that allow detection by fluorescence spectroscopy.

Catechol-appended luminophores have promising properties as functional sensors,^[78–81] redox switches,^[82] photo-^[83,84] and electrocatalysts.^[85] Whilst $[\text{Ru}(\text{bpy})_3]^{2+}$ -type luminophores are still the most commonly studied, $[\text{ReX}(\text{CO})_3(\text{bpy})]$ -type luminophores (with *bpy* = 2,2'-bipyridine and *X* = Br, Cl) have recently emerged as interest-

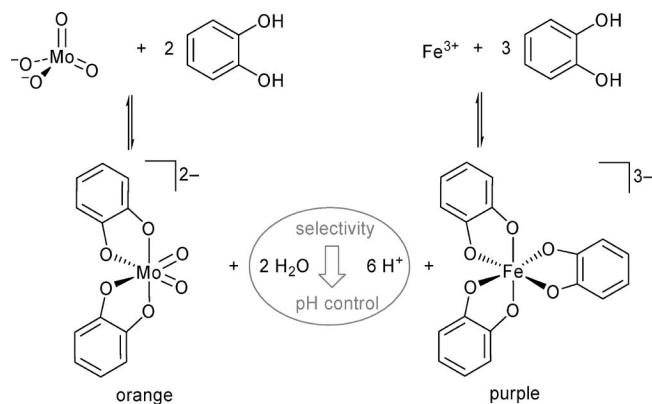


Figure 16. Scheme illustrating the pH-dependence of the reaction of 1,2-dihydroxybenzene (catechol) with molybdate and iron(III).

ing alternatives.^[86–91] In addition, Ru^{II}- and Re^I-based luminophores that incorporate 1,10-phenanthroline instead of 2,2'-bipyridine are increasingly utilised in the field due to their high emission quantum yields and lifetimes.^[92–94]

Because aminochelin showed a high affinity and selectivity for molybdate (see section 1), the siderophore was used as the molybdenum-binding receptor unit in our sensor prototype $[\text{Ru}(\text{bpy})_2(\text{H}_2\text{-L}^7)]^{2+}$ (Figure 17).^[95,96] Amide bond formation between the pendant amine group of aminochelin and 4'-methyl-2,2'-bipyridyl-4-carboxylic acid gives the heteroditopic ligand $\text{H}_2\text{-L}^7$. In $[\text{Ru}(\text{bpy})_2(\text{H}_2\text{-L}^7)]^{2+}$, the bpy unit of $\text{H}_2\text{-L}^7$ is part of the $[\text{Ru}(\text{bpy})_3]^{2+}$ -type luminophore, while the catecholamide unit remains available for molybdate binding. As long as the catecholamide is protonated, the sensor shows intense emission from the $\text{Ru}(\text{d}_\pi) \rightarrow \text{bpy}(\pi^*)$ ³MLCT excited state. Upon deprotonation or molybdenum binding, however, the emission is quenched (Figure 18). The lifetime of the ³MLCT excited state of the sensor decreases from

710 ns, when protonated, to approximately 30 ns, when molybdenum-bound.^[95] Upon addition of molybdate to a buffered solution of $[\text{Ru}(\text{bpy})_2(\text{H}_2\text{-L}^7)]^{2+}$ at pH 5.7 the emission intensity decreases linearly until a molybdenum to sensor ratio of 1:2 is reached (Figure 18). This is consistent with the expected formation of a cis-MoO_2^{2+} complex, in which two catecholamide ligands are coordinated. Between pH 4.8 and 5.8, equimolar amounts of competing cations (Fe^{III} , Cu^{II} , Zn^{II}) and anions (HPO_4^{2-} , ReO_4^-) are tolerated and were found not interfere with the molybdate detection. Although this selectivity for molybdate is promising, the use of the prototype as a chemosensor has several limitations: $[\text{Ru}(\text{bpy})_2(\text{H}_2\text{-L}^7)]^{2+}$ is difficult to synthesise, has limited water solubility and shows a rather high residual emission intensity even in the presence of an excess of molybdate (Figure 18).

To overcome these limitations the second-generation chemosensor $[\text{Re}(\text{bpy})(\text{CO})_3(\text{H}_2\text{-L}^8)]^+$ (Figure 17) was synthesised.^[97] The Re-based luminophore was not only chosen because of its long-lived emission and photochemical stability,^[98] but also because the carbonyl ligands allow the investigation of the quenching mechanism by time-resolved infrared spectroscopy.^[99] The removal of the butylamine-spacer between the luminophore and the catecholamide facilitates the synthesis, increases the hydrophilicity of the sensor and enables electronic coupling between the receptor and the signalling unit. The electron-withdrawing effect of the electron deficient pyridyl group in $\text{H}_2\text{-L}^8$ lowers the pK_a values of the catecholic OH groups, thereby increasing their affinity for molybdenum at low pH. Consequently, the pH range available for detection reaches down to pH values as low as 0.1 and almost complete emission quenching is observed (Figure 19). This is advantageous for a variety of environmental and biological applications, because it allows the direct analysis of acidic metal extracts. The selectivity of the sensor system for oxometalates over transition-metal

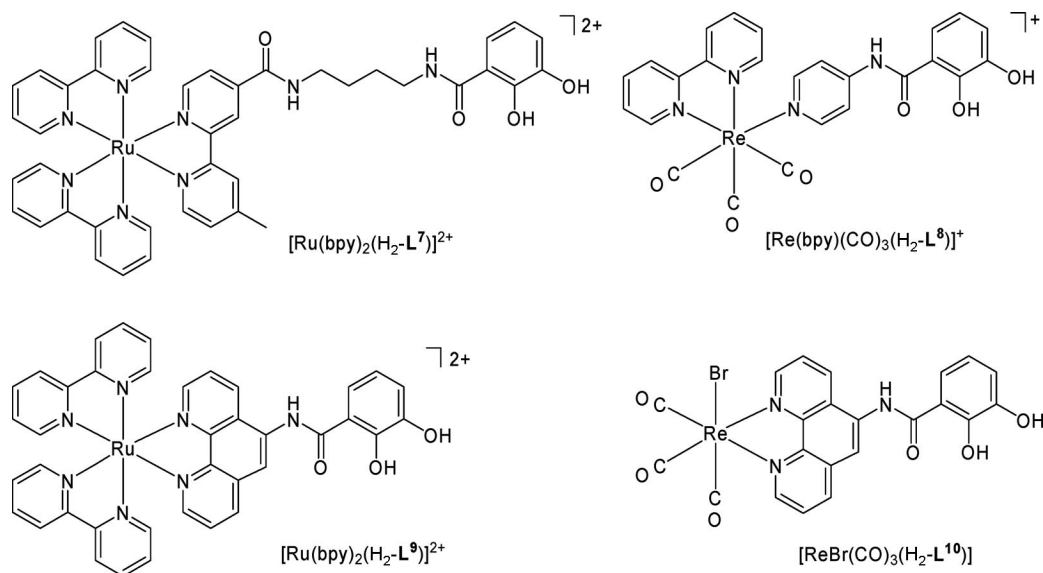


Figure 17. Structures of luminescent sensors for molybdate.

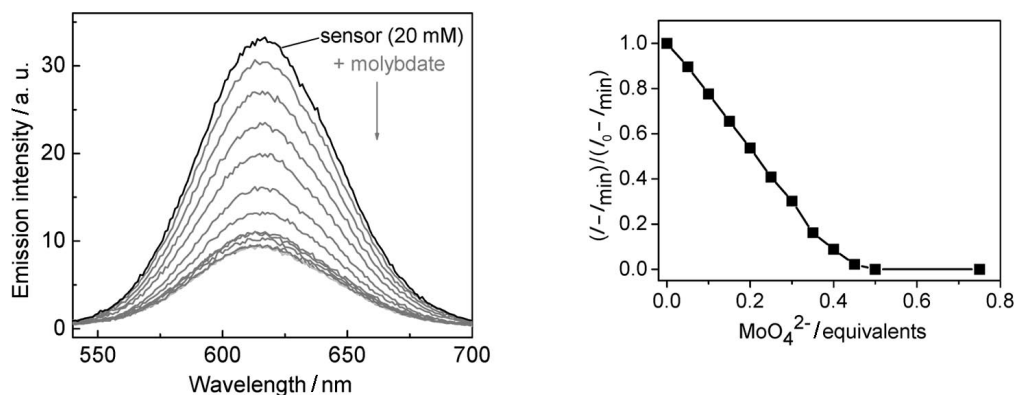


Figure 18. Left: emission spectra of the sensor $[\text{Ru}(\text{bpy})_2(\text{H}_2\text{-L}^7)](\text{PF}_6)_2$ in the presence of increasing amounts of molybdate (aqueous acetonitrile, pH 5.7, $\lambda_{\text{exc}} = 460$ nm). Right: relative emission intensity at 615 nm as a function of molar equivalents of molybdate.

cations and oxoanions of the p-block elements is remarkable. Even the mutually interfering analytes molybdate and tungstate can be differentiated kinetically by taking advantage of the inertness of polyoxotungstates.

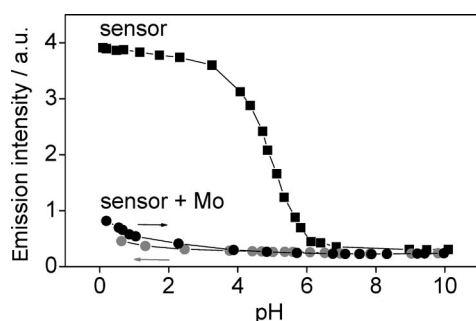


Figure 19. pH-dependence of the emission intensity at 565 nm of the sensor $[\text{Re}(\text{bpy})(\text{CO})_3(\text{H}_2\text{-L}^8)]^+$ (squares) and its Mo complex $[\text{MoO}_2\{\text{Re}(\text{bpy})(\text{CO})_3(\text{L}^8)\}_2]$ [titrated from low to high pH (black dots) and titrated from high to low pH (grey dots)] in aqueous acetonitrile ($\lambda_{\text{exc}} = 370$ nm).

The reaction of $[\text{Re}(\text{bpy})(\text{CO})_3(\text{H}_2\text{-L}^8)]^+$ with molybdate at pH 4 leads to the formation of the *cis*- MoO_2^{2+} -bis(catecholamide) complex $[\text{MoO}_2\{\text{Re}(\text{bpy})(\text{CO})_3(\text{L}^8)\}_2]$, the structure of which could be confirmed by X-ray crystallography.^[99] At pH 4, an apparent overall binding constant $\log \beta_2'$ of $13(\pm 1)$ was obtained and the detection limit was determined to be $55 \mu\text{g L}^{-1}$.^[97]

Furthermore, the heteroditopic ligand $\text{H}_2\text{-L}^9$, which can be coordinated to $\text{Ru}(\text{bpy})_2$ and $\text{ReBr}(\text{CO})_3$ fragments (Figure 17), allowed us to assess how the chemical and photophysical properties of the luminophores influence the metal-binding properties of the catecholamide receptor unit and thereby the performance of the molybdate sensors.^[100] The crystal structures of $[\text{Ru}(\text{bpy})_2(\text{H}_2\text{-L}^9)]^{2+}$ and $[\text{ReBr}(\text{CO})_3(\text{H}_2\text{-L}^9)]$ are shown in Figure 20. In both cases, $\text{H}_2\text{-L}^9$ is almost planar and an intramolecular hydrogen bond is formed between the amide NH and the O atom in the *ortho*-position of the catecholamide unit. As expected,

the deprotonation of the *ortho*-OH group in the positively charged complex $[\text{Ru}(\text{bpy})_2(\text{H}_2\text{-L}^9)]^{2+}$ is easier ($\text{p}K_{\text{a}} = 4.5$) than in the neutral complex $[\text{ReBr}(\text{CO})_3(\text{H}_2\text{-L}^9)]$ ($\text{p}K_{\text{a}} = 5.75$). Although both complexes function as molybdate and vanadate sensors, the lower $\text{p}K_{\text{a}}$ value and the higher emission intensity of $[\text{Ru}(\text{bpy})_2(\text{H}_2\text{-L}^9)]^{2+}$ gives rise to a detection limit that is almost an order of magnitude lower than that achieved with $[\text{ReBr}(\text{CO})_3(\text{H}_2\text{-L}^9)]$ (Table 2) and three orders of magnitude lower than the one reported for the colorimetric determination of molybdate with catechol.^[77] The detection limit for molybdate is similar to those reported for highly fluorescent organic reagents, such as Alizarin Red S ($100 \mu\text{g L}^{-1}$)^[101] or bathophenanthroline disulfonate ($10 \mu\text{g L}^{-1}$)^[102] but still higher than that reported for 2-hydroxy-1-naphthaldehyde-8-aminoquinoline ($0.08 \mu\text{g L}^{-1}$).^[103] In contrast to organic fluorophores, $[\text{Ru}(\text{bpy})_2(\text{H}_2\text{-L}^9)]^{2+}$ and $[\text{ReBr}(\text{CO})_3(\text{H}_2\text{-L}^9)]$, however, show long-lived emission and large differences between excitation and emission wavelengths. These properties can be used to eliminate biological background fluorescence. The presence of equimolar amounts of biologically relevant cations, such as Mn^{II} , Fe^{III} , Co^{II} , Ni^{II} and Zn^{II} , and oxoanions, including SO_4^{2-} and HPO_4^{2-} , do not interfere with molybdate and vanadate detection. Perrhenate, which is diagonally related to molybdate in the periodic Table, was also shown not to quench the emission of $[\text{Ru}(\text{bpy})_2(\text{H}_2\text{-L}^9)]^{2+}$ and $[\text{ReBr}(\text{CO})_3(\text{H}_2\text{-L}^9)]$.

Further applications of metal complexes with pendant catecholate groups are emerging, for example based on the observation that catecholate units interact strongly with the surface of early transition-metal oxides, such as TiO_2 . They can thus be used for the immobilisation of photosensitisers,^[104,105] catalysts,^[106] or fluorophores.^[107] Interestingly, a polymeric ligand with pendant catecholate groups has recently been used in the solubilisation and functionalisation of inert MoS_2 nanoparticles.^[108] This study is of relevance with regard to the siderophore-mediated mobilisation of molybdenum in the environment, as it suggests that catecholamides might be able to sequester molybdenum from otherwise inaccessible sources.

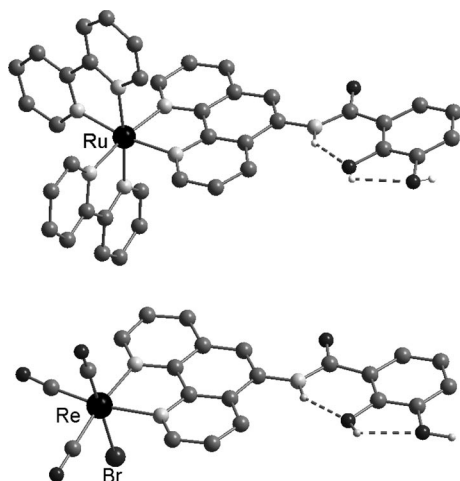


Figure 20. Ball-and-stick representation of the molecular structures of $[\text{Ru}(\text{bpy})_2(\text{H}_2\text{-L}^9)]^{2+}$ (top) and $[\text{ReBr}(\text{CO})_3(\text{H}_2\text{-L}^9)]$ (bottom). O black, N light grey, C grey, H white, H atoms, apart from OH and NH, omitted for clarity.

Table 2. Comparison of the pK_a values of the *ortho*-OH group and the detection limits for molybdate for the three second generation sensor systems.

Sensor	pK_a of <i>ortho</i> -OH	Detection limit
$[\text{ReBr}(\text{CO})_3(\text{H}_2\text{-L}^9)]$	5.75	$315 \mu\text{g L}^{-1}$
$[\text{Re}(\text{bpy})(\text{CO})_3(\text{H}_2\text{-L}^8)]^+$	4.9	$55 \mu\text{g L}^{-1}$
$[\text{Ru}(\text{bpy})_2(\text{H}_2\text{-L}^9)]^{2+}$	4.5	$43 \mu\text{g L}^{-1}$

Summary and Perspectives

It is now well established that ligands with catecholamide-based binding sites form very stable *cis*- MoO_2^{2+} complexes. This finding is biologically important, because molybdate competes with iron(III) for the catecholamide siderophores secreted by microorganisms, as studied in detail for the siderophores of the nitrogen-fixing bacterium *Azotobacter vinelandii*. Whether the molybdenum–siderophore complexes formed are taken up by the cells as such, either via specific molybdenum–siderophore transporters or by use of the iron-uptake system, remains to be investigated. As an essential component of the conventional nitrogenase, molybdenum plays a crucial role in the fixation of atmospheric nitrogen and thus ultimately in the improvement of soil fertility and crop production. In this context, further insights into ways to support and optimise bacterial molybdenum and iron uptake are urgently required.

The synthesis and characterisation of molybdenum(VI)–siderophore complexes and structurally related model compounds helped to establish catecholamides as suitable ligands for the self-assembly of supramolecular complexes, an area that has subsequently attracted much attention. In addition, the *cis*- MoO_2^{2+} unit was shown to give rise to structures that are not easily accessible with other metal ions. Because the two oxido ligands can accept hydrogen bonds and coordinate to counterions, they provide the opportunity to control the spatial arrangement and packing of the complexes in hierarchical supramolecular systems. This

possibility, together with the chirality of the molybdenum centre in *cis*- MoO_2^{2+} –catecholamide complexes, can be exploited in the design of even larger chiral structures. This opens up exciting new avenues for future studies.

The high affinity of catecholamides for molybdenum has also provided the inspiration for the development of luminescent chemosensors for oxometalates, such as molybdate, vanadate and tungstate. The sensors consist of luminescent Re- or Ru-based signalling units with pendant catecholamide receptor units. This modular design facilitates the tuning and optimisation of their properties. Future perspectives in this area include the increase of the water solubility of the molecular sensors or their immobilisation, for example on fibre-optic tips.

Acknowledgments

I would like to thank all the students, post-docs and collaborators who have contributed to this work over the years. Financial support from the Engineering and Physical Sciences Research Council, the Biotechnology and Biological Sciences Research Council, Deutsche Forschungsgemeinschaft, Verband der Chemischen Industrie and the University of York is gratefully acknowledged. I would also like to thank the European Commission Marie Curie action and European Cooperation in Science and Technology action D35 for supporting research and a short-term scientific mission.

- [1] H. Sigel, A. Sigel (Eds.), *Metal Ions in Biological Systems, Vol. 39, Molybdenum and Tungsten: Their Roles in Biological Processes*, Marcel Dekker, New York, **2002**.
- [2] http://www.imoa.info/moly_uses/moly_chemistry_uses/molybdenum_chemistry_uses.html, last accessed 08/04/2009.
- [3] I. J. R. Da Silva, R. P. J. Williams, *The Biological Chemistry of the Elements*, Clarendon Press, Oxford, **1991**, ch. 17.
- [4] K. S. Smith, L. S. Balistreri, S. M. Smith, R. C. Severson in *Molybdenum in Agriculture* (Ed.: U. C. Gupta), Cambridge University Press, **1997**, ch. 3.
- [5] M. Kaupp, *Angew. Chem. Int. Ed.* **2001**, *40*, 3534.
- [6] D. C. Brower, J. L. Templeton, D. M. P. Mingos, *J. Am. Chem. Soc.* **1987**, *109*, 5203.
- [7] W. P. Griffith, T. D. Wickings, *J. Chem. Soc. A* **1968**, 400.
- [8] W. P. Griffith, H. I. S. Nogueira, B. C. Parkin, R. N. Sheppard, A. J. P. White, D. J. Williams, *J. Chem. Soc., Dalton Trans.* **1995**, 1775.
- [9] E. I. Stiefel, B. K. Burgess, S. Wherland, W. E. Newton, J. L. Corbin, G. D. Watt in *Nitrogen Fixation* (Eds.: W. E. Newton, W. H. Orme-Johnson), University Park Press, Baltimore, **1980**, p. 216.
- [10] W. Page, M. von Tigerström, *J. Bacteriol.* **1982**, *149*, 237.
- [11] A. S. Cornish, W. J. Page, *BioMetals* **1995**, *8*, 332.
- [12] A.-K. Duhme, R. C. Hider, M. J. Naldrett, R. N. Pau, *J. Biol. Inorg. Chem.* **1998**, *3*, 520.
- [13] A. M. Grunden, K. T. Shanmugam, *Arch. Microbiol.* **1997**, *168*, 345.
- [14] R. N. Pau, D. M. Lawson in *Metal Ions in Biological Systems, Vol. 39, Molybdenum and Tungsten: Their Roles in Biological Processes* (Eds.: H. Sigel, A. Sigel), Marcel Dekker, New York, **2002**, ch. 2.
- [15] R. N. Pau in *Genetics and Regulation of Nitrogen Fixation in Free-Living Bacteria* (Eds.: W. Klipp, B. Masepohl, J. R. Gallon, W. E. Newton), Kluwer Academic Publishers, Dordrecht, **2004**, p. 225.
- [16] K. Taraz, G. Ehlert, K. Geisen, H. Budzikiewicz, *Z. Naturforsch.* **1990**, *45b*, 1327.

- [17] A.-K. Duhme, R. C. Hider, H. H. Khodr, *Chem. Ber./Recueil* **1997**, *130*, 969.
- [18] A. S. Cornish, W. J. Page, *Microbiology* **1998**, *144*, 1747.
- [19] R. C. Scarrow, D. J. Ecker, C. Ng, S. Liu, K. N. Raymond, *Inorg. Chem.* **1991**, *30*, 900.
- [20] A. S. Cornish, W. J. Page, *Appl. Environ. Microbiol.* **2000**, *66*, 1580.
- [21] T. Wichard, J.-P. Bellenger, A. Loison, A. M. L. Kraepiel, *Environ. Sci. Technol.* **2008**, *42*, 2408.
- [22] J.-P. Bellenger, T. Wichard, A. B. Kustka, A. M. L. Kraepiel, *Nat. Geosci.* **2008**, *1*, 243.
- [23] M. Albrecht, S. J. Franklin, K. N. Raymond, *Inorg. Chem.* **1994**, *33*, 5785.
- [24] R. C. Hider, *Struct. Bonding (Berlin)* **1984**, *58*, 25.
- [25] A.-K. Duhme-Klair, *Habilitationsschrift*, Westfälische Wilhelms-Universität Münster, Germany, **1999**, ch. 3.
- [26] J.-P. Bellenger, F. Arnaud-Neu, Z. Asfari, S. C. B. Myneni, E. I. Stiefel, A. M. L. Kraepiel, *J. Biol. Inorg. Chem.* **2007**, *12*, 367.
- [27] J. R. Telford, K. N. Raymond, *Inorg. Chem.* **1998**, *37*, 4578.
- [28] W. Page, M. Huyer, *J. Bacteriol.* **1984**, *158*, 496.
- [29] A.-K. Duhme, R. C. Hider, H. Khodr, *BioMetals* **1996**, *9*, 245.
- [30] L. J. Liermann, R. L. Guynn, A. Anbar, S. L. Brantley, *Chem. Geol.* **2005**, *220*, 285.
- [31] S. H. Behrens, D. G. Grier, *J. Chem. Phys.* **2001**, *115*, 6716.
- [32] H. H. Khodr, R. C. Hider, A.-K. Duhme-Klair, *J. Biol. Inorg. Chem.* **2002**, *7*, 891.
- [33] Single crystals of $[\text{MoO}_2(\text{H-aminochelin})_2]$ were obtained by slow diffusion of ethanol into a concentrated solution of the complex in DMSO. The complex crystallises in the orthorhombic space group *Pbcn* (*Z* = 4) with cell parameters *a* = 12.601(3), *b* = 15.883(3) and *c* = 13.579(3). The butyl chains in the structure are heavily disordered. Because the crystals $[\text{MoO}_2(\text{H-aminochelin})_2]$ diffracted only weakly and the quality of the collected data set is limited the disorder could not be resolved completely. A final *R*₁ value of 0.12 was obtained.
- [34] W. J. Page, M. von Tigerström, *J. Gen. Microbiol.* **1988**, *134*, 453.
- [35] Review on ferric iron reductases: I. Schroder, E. Johnson, S. de Vries, *FEMS Microbiol. Rev.* **2003**, *27*, 427.
- [36] Recent review on siderophore-mediated iron uptake: M. Miethke, M. A. Marahiel, *Microbiol. Mol. Biol. Rev.* **2007**, *71*, 413.
- [37] B. F. Matzanke, S. Anemüller, V. Schnemann, A. X. Trautwein, K. Hantke, *Biochemistry* **2004**, *43*, 1386.
- [38] V. Sedlacek, R. J. M. van Spanning, I. Kucera, *Microbiology* **2009**, *155*, 1294.
- [39] A.-K. Duhme-Klair, D. C. L. de Alwis, F. A. Schultz, *Inorg. Chim. Acta* **2003**, *351*, 150.
- [40] J. P. Robinson, J. V. McArdle, *J. Inorg. Nucl. Chem.* **1981**, *43*, 1951.
- [41] P. T. Pienkos, W. J. Brill, *J. Bacteriol.* **1981**, *145*, 743.
- [42] A.-K. Duhme, W. Meyer-Klaucke, D. J. White, L. Delarbre, L. A. Mitchenall, R. N. Pau, *J. Biol. Inorg. Chem.* **1999**, *4*, 588.
- [43] D. M. Lawson, C. E. Williams, L. A. Mitchenall, R. N. Pau, *Structure* **1998**, *6*, 1519.
- [44] Y. Hu, S. Reck, R. P. Gunsalus, D. C. Rees, *Nat. Struct. Biol.* **1997**, *4*, 73.
- [45] J. Wiethaus, A. Wirsing, F. Narberhaus, B. Masepohl, *J. Bacteriol.* **2006**, *188*, 8441.
- [46] A. Balan, C. Santacruz-Perez, A. Moutran, L. C. Souza Ferreira, G. Neshich, J. A. R. Goncalves Barbosa, *Biochim. Biophys. Acta* **2008**, *1784*, 393.
- [47] J. Imperial, M. Hadi, N. K. Amy, *Biochim. Biophys. Acta* **1998**, *1370*, 337.
- [48] L. E. Wasylenko, A. D. Anbar, L. J. Liermann, R. Mathur, G. W. Gordon, S. L. Brantley, *J. Anal. At. Spectrom.* **2007**, *22*, 905.
- [49] A. Müller, A. J. Wilkinson, K. S. Wilson, A.-K. Duhme-Klair, *Angew. Chem. Int. Ed.* **2006**, *45*, 5132.
- [50] A. M. L. Kraepiel, J. P. Bellenger, T. Wichard, F. M. M. Morel, *Biometals* **2009**, 573.
- [51] W. P. Griffith, H. I. S. Nogueira, B. C. Parkin, R. N. Sheppard, A. J. P. White, D. J. Williams, *J. Chem. Soc., Dalton Trans.* **1995**, 1775.
- [52] M. Albrecht, M. Baumert, J. Klankermayer, M. Kogej, C. A. Schalley, R. Fröhlich, *Dalton Trans.* **2006**, 4395.
- [53] A.-K. Duhme, *J. Chem. Soc., Dalton Trans.* **1997**, 773.
- [54] M. Albrecht, *Chem. Soc. Rev.* **1998**, *172*, 281.
- [55] M. Albrecht, *Chem. Rev.* **2001**, *101*, 3457.
- [56] D. L. Caulder, K. N. Raymond, *J. Chem. Soc., Dalton Trans.* **1999**, 1185.
- [57] D. L. Caulder, K. N. Raymond, *Acc. Chem. Res.* **1999**, *32*, 975.
- [58] M. J. Hannon, L. J. Childs, *Supramol. Chem.* **2004**, *16*, 7.
- [59] A.-K. Duhme, Z. Dauter, R. C. Hider, S. Pohl, *Inorg. Chem.* **1996**, *35*, 3059.
- [60] E. J. Enemark, T. D. P. Stack, *Angew. Chem. Int. Ed. Engl.* **1995**, *34*, 996.
- [61] M. Albrecht, S. Kotila, *Angew. Chem. Int. Ed. Engl.* **1995**, *34*, 996.
- [62] B. Kersting, M. Meyer, R. E. Powers, K. N. Raymond, *J. Am. Chem. Soc.* **1996**, *118*, 7221.
- [63] A.-K. Duhme, *Z. Anorg. Allg. Chem.* **1998**, *624*, 1922.
- [64] A.-K. Duhme-Klair, G. Vollmer, C. Mars, R. Fröhlich, *Angew. Chem. Int. Ed.* **2000**, *39*, 1626.
- [65] A.-K. Duhme, S. C. Davies, D. L. Hughes, *Inorg. Chem.* **1998**, *37*, 5380.
- [66] I. Prevot-Halter, J. Weiss, *New J. Chem.* **1998**, *22*, 869.
- [67] M. Albrecht, P. Stortz, J. Runsink, P. Weis, *Chem. Eur. J.* **2004**, *10*, 3657.
- [68] K. Kustin, S.-T. Liu, *J. Am. Chem. Soc.* **1973**, *95*, 2487.
- [69] C.-M. Liu, E. Nordlander, D. Schmeh, R. Shoemaker, C. G. Pierpont, *Inorg. Chem.* **2004**, *43*, 2114.
- [70] C. G. Pierpont, R. M. Buchanan, *Coord. Chem. Rev.* **1981**, *38*, 45.
- [71] C. G. Pierpont, C. W. Lange, *Prog. Inorg. Chem.* **1994**, *41*, 331.
- [72] E. Farkas, H. Csoka, *J. Inorg. Biochem.* **2002**, *89*, 219.
- [73] J. Mason, *Toxicology* **1986**, *42*, 99.
- [74] J. Kuper, A. Llamas, H.-J. Hecht, R. R. Mendel, G. Schwarz, *Nature* **2004**, *430*, 803.
- [75] V. E. Shih, I. F. Abroms, J. L. Johnson, M. Carney, R. Mandell, R. M. Robb, J. P. Cloherty, K. V. Rajagopalan, *N. Engl. J. Med.* **1977**, *297*, 1022.
- [76] C. Kisker, H. Schindelin, A. Pacheco, W. A. Wehbi, R. M. Garrett, K. V. Rajagopalan, J. H. Enemark, D. C. Rees, *Cell* **1997**, *91*, 973.
- [77] F. D. Snell, *Photometric and Fluorometric Methods of Analysis, Metals, Part 2*, John Wiley & Sons, New York, **1978**, p. 1296.
- [78] P. D. Beer, *Chem. Commun.* **1996**, 689.
- [79] I. Costa, L. Fabbri, P. Pallavicini, A. Poggi, A. Zani, *Inorg. Chim. Acta* **1998**, *275–276*, 117.
- [80] L. O'Bian, M. Duati, S. Rau, A. L. Guckian, T. E. Keyes, N. M. O'Boyle, A. Serr, H. Görls, J. G. Vos, *Dalton Trans.* **2004**, 514.
- [81] D. Jose, P. Kar, D. Koley, B. Ganguly, W. Thiel, H. N. Ghosh, A. Das, *Inorg. Chem.* **2007**, *46*, 5576.
- [82] V. Goulle, A. Harriman, J.-M. Lehn, *J. Chem. Soc., Chem. Commun.* **1993**, 1034.
- [83] B. Whittle, N. S. Everest, C. Howard, M. D. Ward, *Inorg. Chem.* **1995**, *34*, 2025.
- [84] A. D. Shukla, B. Whittle, H. C. Bajaj, A. Das, M. D. Ward, *Inorg. Chim. Acta* **1999**, *285*, 89.
- [85] G. D. Storrier, K. Takada, H. D. Abruna, *Inorg. Chem.* **1999**, *38*, 559.
- [86] K. S. Schanze, D. B. MacQueen, T. A. Perkins, L. A. Cabana, *Coord. Chem. Rev.* **1993**, *122*, 63.
- [87] S.-S. Sun, A. J. Lees, *Coord. Chem. Rev.* **2002**, *230*, 171.
- [88] J. D. Lewis, R. N. Perutz, J. N. Moore, *Chem. Commun.* **2000**, 1865.

- [89] M. Busby, P. Matousek, M. Towrie, I. P. Clark, M. Motevalli, F. Hartl, A. Vlček Jr, *Inorg. Chem.* **2004**, *43*, 4523.
- [90] M. Cattaneo, F. Fagalde, C. D. Borsarelli, N. E. Katz, *Inorg. Chem.* **2009**, *48*, 3012.
- [91] A. Cannizzo, A. M. Blanco-Rodriguez, A. El Nahhas, C. Sebera, S. Zalis, A. Vlček Jr, M. Chergui, *J. Am. Chem. Soc.* **2008**, *130*, 8967.
- [92] E. M. Kober, T. J. Meyer, *Inorg. Chem.* **1985**, *24*, 106.
- [93] V. P. Boricha, S. Patra, Y. S. Chouhan, P. Sanavada, E. Suresh, P. Paul, *Eur. J. Inorg. Chem.* **2009**, 1256.
- [94] C. Shih, A. K. Museth, M. Abrahamsson, A. M. Blanco-Rodriguez, A. J. Di Bilio, J. Sudhamsu, B. R. Crane, K. L. Ronayne, M. Towrie, A. Vlček Jr, J. H. Richards, J. R. Winkler, H. B. Gray, *Science* **2008**, *320*, 1760.
- [95] S. B. Jedner, R. J. James, R. N. Perutz, A.-K. Duhme-Klair, *J. Chem. Soc., Dalton Trans.* **2001**, 2327.
- [96] S. B. Jedner, R. N. Perutz, A.-K. Duhme-Klair, *Z. Anorg. Allg. Chem.* **2003**, *629*, 2421.
- [97] A. F. A. Peacock, H. D. Batey, C. Rändler, A. C. Whitwood, R. N. Perutz, A.-K. Duhme-Klair, *Angew. Chem. Int. Ed.* **2005**, *44*, 1712.
- [98] K. S. Schanze, D. B. MacQueen, T. A. Perkins, L. A. Cabana, *Coord. Chem. Rev.* **1993**, *122*, 63.
- [99] V. A. Corden, N. Reddig, K. Ronayne, M. Towrie, R. N. Perutz, A.-K. Duhme-Klair, manuscript in preparation.
- [100] H. D. Batey, A. C. Whitwood, A.-K. Duhme-Klair, *Inorg. Chem.* **2007**, *46*, 6516.
- [101] C. C. Blanco, A. G. Campana, F. A. Barrero, M. R. Ceba, *Anal. Chim. Acta* **1993**, *283*, 213.
- [102] B. K. Pal, K. A. Singh, K. Dutta, *Talanta* **1992**, *39*, 971.
- [103] C. Jiang, J. Wang, F. He, *Anal. Chim. Acta* **2001**, *439*, 307.
- [104] C. R. Rice, M. D. Ward, M. K. Nazeeruddin, M. Grätzel, *New J. Chem.* **2000**, *24*, 651.
- [105] S. G. Abuabara, C. W. Cady, J. B. Baxter, C. A. Schmuttenmaer, R. H. Crabtree, G. W. Brudwig, V. S. Batista, *J. Phys. Chem. C* **2007**, *111*, 11982.
- [106] N. T. Lucas, J. M. Hook, A. M. McDonagh, S. B. Colbran, *Eur. J. Inorg. Chem.* **2005**, 496.
- [107] M. N. Tahir, M. Eberhardt, P. Theato, S. Faiß, A. Janshoff, T. Gorelik, U. Kolb, W. Tremel, *Angew. Chem. Int. Ed.* **2006**, *45*, 908.
- [108] M. N. Tahir, N. Zink, M. Eberhardt, H. A. Therese, U. Kolb, P. Theato, W. Tremel, *Angew. Chem. Int. Ed.* **2006**, *45*, 4809.

Received: May 7, 2009

Published Online: July 24, 2009